Redox Biology 20 (2019) 526–532

Contents lists available at ScienceDirect

Redox Biology

journal homepage: www.elsevier.com/locate/redox

Research paper

Proteomic analysis of microbial induced redox-dependent intestinal signaling

Jason D. Matthews[a], April R. Reedy[a], Huixia Wu[a], Benjamin H. Hinrichs[a], Trevor M. Darby[b], Caroline Addis[b], Brian S. Robinson[a], Young-Mi Go[c], Dean P. Jones[c], Rheinallt M. Jones[b], Andrew S. Neish[a,*]

[a] Department of Pathology, Emory University School of Medicine, Atlanta, GA, USA
[b] Department of Pediatrics, Emory University School of Medicine, Atlanta, GA, USA
[c] Department of Medicine, Emory University School of Medicine, Atlanta, GA, USA

A B S T R A C T

Intestinal homeostasis is regulated in-part by reactive oxygen species (ROS) that are generated in the colonic mucosa following contact with certain lactobacilli. Mechanistically, ROS can modulate protein function through the oxidation of cysteine residues within proteins. Recent advances in cysteine labeling by the Isotope Coded Affinity Tags (ICATs) technique has facilitated the identification of cysteine thiol modifications in response to stimuli. Here, we used ICATs to map the redox protein network oxidized upon initial contact of the colonic mucosa with *Lactobacillus rhamnosus* GG (LGG). We detected significant LGG-specific redox changes in over 450 proteins, many of which are implicated to function in cellular processes such as endosomal trafficking, epithelial cell junctions, barrier integrity, and cytoskeleton maintenance and formation. We particularly noted the LGG-specific oxidation of Rac1, which is a pleiotropic regulator of many cellular processes. Together, these data reveal new insights into lactobacilli-induced and redox-dependent networks involved in intestinal homeostasis.

1. Introduction

The gastrointestinal mucosa functions as a dynamic barrier separating the luminal contents, including a vast microbiota, from the underlying systemic compartments. Despite the potential threat of a myriad of viable prokaryotes and their products, some bacterial members of the intestinal microbiota also serve many diverse beneficial functions, ranging from the competitive exclusion of pathogenic microorganisms [1], to influencing cancer immunotherapy [14]. In addition, experiments have shown a role of the microbiota in epithelial proliferation and wound recovery post injury [2,43,44]. Furthermore, exogenously administered viable bacteria, known as 'probiotics', can dampen inflammation, improve barrier function and promote reparative responses in vitro, and have shown promise as therapy in inflammatory and developmental disorders of the intestinal tract [16,44,9]. Additionally, fecal microbiota transplantation, which involves direct intra colonic instillation of fecal and/or bacterial suspensions, has become a first line therapy for C. difficile infection and is being explored in multiple other intestinal conditions [32,7,8].

Several lactobacilli strains, which are naturally occurring members of the microbiota and commonly used probiotics, have been shown to generate and/or induce reactive oxygen species (ROS) production [24,36,37]. We reported that certain strains of lactobacilli, in particular *Lactobacillus rhamnosus* GG (LGG) can induce rapid, and non-microbicidal generation of ROS within colonic epithelial cells [20]. This evolutionarily conserved generation of ROS mediates cell signaling responses in mammalian cultured cells, in invertebrate models, and in the murine model [17,18,22,24,25,3,36,37,39,41,42]. ROS were initially described as functioning in the bactericidal responses of neutrophils, where high levels of ROS are generated by the catalytic activity of the NADPH oxidase (Nox) enzymes, Nox2/gp120phox, also known as 'respiratory burst' [23]. Subsequent research discovered paralogs of Nox enzymes expressed in non-phagocytic tissues, with Nox1 strongly expressed in intestinal epithelia [26]. Indeed, controlled generation of ROS by Nox enzymes has been reported as a response to receptor activation by various hormones, cytokines, and growth factors, which thereafter activate multiple downstream cell signaling transduction pathways [29–31,35,6].

ROS, in particular H_2O_2, affects signal transduction pathways via their ability to rapidly and reversibly oxidize cysteine residues in specific target proteins, usually regulatory enzymes, thus allowing for graded perception of intracellular ROS concentrations and control of critical steps in signal transduction pathways [19,21,34,35]. The current paradigm holds that redox signaling occurs via the effects of "sensor" proteins that harbor oxidant-sensitive cysteine residues that are rapidly and reversibly modified by oxidative stress. There are over

* Correspondence to: Department of Pathology, Emory University School of Medicine, Room 105A, Whitehead Bldg., 615 Michael Street, Atlanta, GA 30322, USA.
E-mail address: aneish@emory.edu (A.S. Neish).

https://doi.org/10.1016/j.redox.2018.11.011
Received 30 August 2018; Received in revised form 13 November 2018; Accepted 15 November 2018
Available online 22 November 2018

214,000 cysteine residues in the human proteome that may potentially be modified by cellular redox changes. However, current in silico bioinformatics methods offer no information about which cysteine residues are functionally active in redox signaling. One technique currently used to discover oxidant-sensitive cysteine residues is a proteomic approach called isotope-coded affinity tags (ICAT), which differentially labels individual cysteine residues in a binary fashion depending on the cysteine redox state (oxidized or reduced), and allows for both the identification and a measure of the relative oxidation level of the active cysteine upon exposure to stimuli [11,12]. Thus, ICAT is an ideal method to assess the influence of ROS generated within cells in response to lactobacilli contact with the intestinal mucosa. In this study, we define a subset of proteins and corresponding cysteine residues that are altered by LGG-induced cellular ROS. We also infer how these proteins may function in cellular processes that are known to be influenced by LGG contact with colonic epithelial cells. Together, these data reveal new insights into lactobacilli regulation of the redox-dependent networks involved in intestinal homeostasis.

2. Results and discussion

Previously we showed that loss of Nox-1 enzyme by genetic knockout in mice resulted in the loss of LGG induced ROS in the epithelium upon contact [3]. Similar Nox-1 mediated results were observed for Lactobacillus plantarum in drosophila [18], suggesting that these increases in ROS leads to oxidation of key cysteine residues that modify protein confirmation and cellular function as depicted in Fig. 1A. Additionally, a recent report has shown that certain strains of lactobacilli generate hydrogen peroxide [37], indicating that some cellular protein oxidation is caused by ROS produced by the luminal bacteria themselves. We tested the supernatants from overnight cultures of several strains of lactobacilli, including two of our separate lab stocks of LGG (ATCC 53103), and found that while strains of *Lactobacillus acidophilus* or *Lactobacillus gasseri* produced high levels of hydrogen peroxide, in comparison LGG by itself did not produce high levels of hydrogen peroxide relative to the untreated control (Fig. 1B). These data indicate that the ROS produced in the intestinal epithelium occur upon specific contact with LGG.

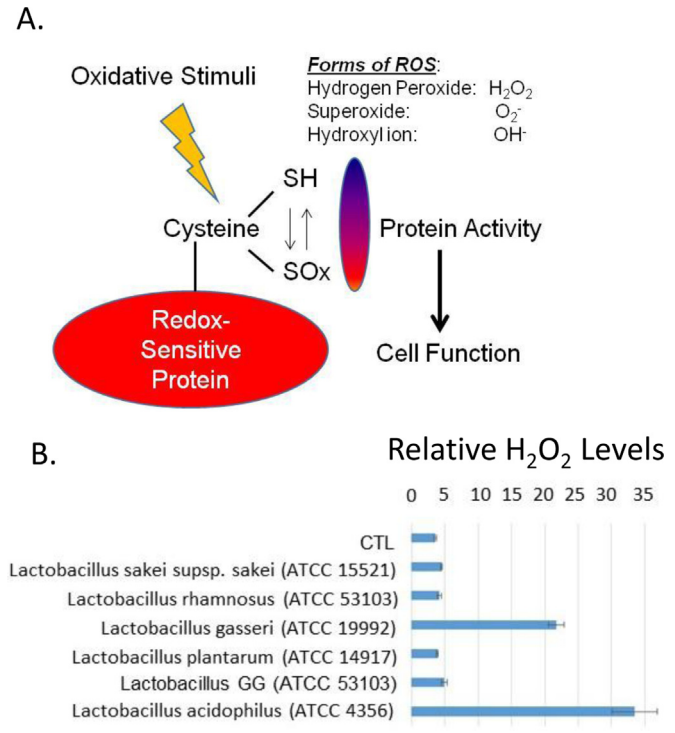

Fig. 1. Cellular or bacterial derived ROS can alter protein function. (A) Schematic of cysteine oxidation to regulate cell function. (B) Various strains of Lactobacillus were tested for their ability to produce hydrogen peroxide. Bacteria were grown in overnight cultures and the supernatants tested against a negative PBS control for the relative abundance of hydrogen peroxide in a 96-well plate using a ROS-GLO kit. A luminometer was used to quantify the levels of hydrogen peroxide.

While the downstream physiological effects of enhanced proliferation, migration and homeostasis have been observed upon LGG administration and subsequent ROS production [18,27,3], the signaling events driving these cellular processes are still largely unknown. By using ICAT labeling coupled with mass spectrometry, our goal was to identify key epithelial cell proteins and their active cysteine residues that are responsible for mediating the redox signaling induced by LGG.

First, we examined ROS production and its global effect on protein oxidation in vitro using SKCO15 cells, which is a human intestinal epithelial cell (IEC) line. We chose the attenuated *E. coli* K12 DH5 strain as a negative bacterial control for our experiments because it does not induce ROS in the epithelium upon immediate contact (as observed against a PBS control, Fig. 2A), and thus serves as a control for cellular responses that occur from non-specific bacterial exposure. Consistent with previous reports, IECs exposed to 10^8 CFU/mL of LGG for 15 min exhibited elevated levels of the ROS-reactive HydroCy3 fluorescence, compared to PBS and *E. coli* as controls (Fig. 2A). Thus, subsequent experiments employed *E.coli* as a bacterial negative control. Next, we measured the global cysteine oxidation state using a thiol-specific Thiol Tracker™ probe whereby oxidized thiols on cysteine residues do not react (and emit fluorescence) with the Thiol Tracker™ probe. Consistently, we detected decreased relative Thiol Tracker™ fluorescence in SKCO15 cells that were in contact with LGG, indicating a higher level of protein oxidation (7-fold increase) compared to cells in contact with *E. coli* (Fig. 2B). To biochemically assess the levels of global protein oxidation within SKCO15 cells in response to LGG, we performed protein-iodoacetamide-biotinylation (BIAM) pull-down assays, whereby reduced protein thiols are biotinylated and then captured using streptavidin agarose beads. These captured biotinylated proteins are then subjected to Western blot analysis. Using HRP conjugated streptavidin as a probe on the Western blot, biotinylated proteins can be detected. Thus, the measured amounts of incorporated biotin into proteins are inversely proportional to the amount of oxidized proteins within the cell following cellular contact with *E.coli* and LGG. Accordingly, we show that fewer biotinylated proteins were captured from SKCO15 cells following contact with LGG compared to following contact with *E. coli*, indicating higher protein oxidation levels within the LGG-contacted cells (equal levels of protein loading shown by blotting for calnexin as a loading control, Fig. 2C, right). Indeed, quantitative analysis of the decrease in BIAM pull-down signal between cultures exposed to LGG or *E. coli* revealed that LGG contact increased global oxidation of cellular proteins by approximately 30% (Fig. 2C, left). Collectively, these assays reflect extensive oxidation at the protein level in SKCO15 cells exposed to LGG.

Closer analysis of the HydroCy3 fluorescence in SKCO15 cells contacted by LGG revealed that HydroCy3 fluorescence co-localized with lysosomes in cells (Fig. 2D). This was in contrast to SKCO15 cells contacted by *E. coli*, which did not exhibit similar co-localization. The HydroCy3 signal does not conjugate with proteins, and thus its accumulation is in the subcellular compartments with higher ROS levels irrespective of protein localization. These observations are significant because it has been reported that Nox1 undergoes endocytosis at the plasma membrane, and gains activity upon cellular internalization of the endocytic vesicle [30,35]. For example, IL1-β and TNFα are thought to increase ROS production by promoting the endosomal internalization of Nox1 [30,35]. Current literature suggests that the endosomes move into the cytoplasm and act as “redoxosomes” capable of oxidizing proteins in close proximity to the vesicle [35,38]. Consistent with these reports, the observed increases in HyrdoCy3 fluorescence in the

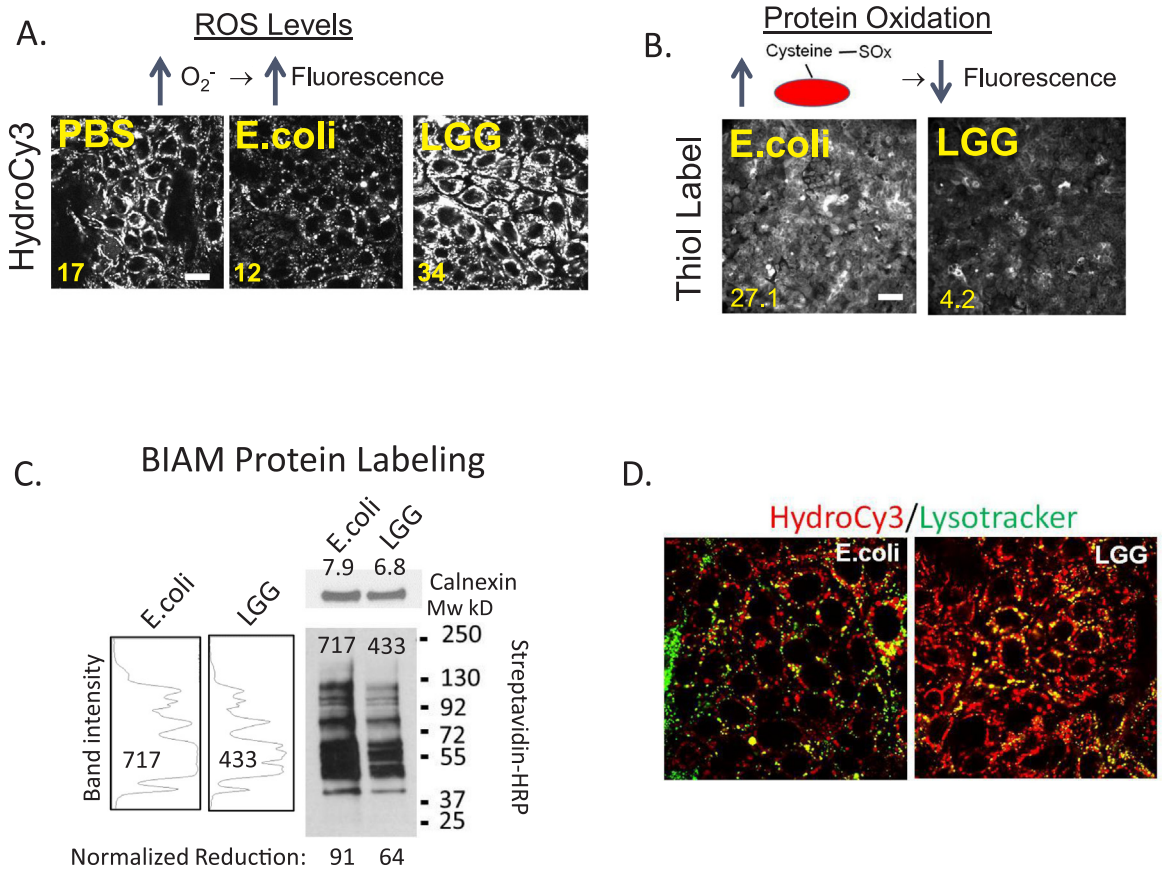

Fig. 2. LGG induces ROS that oxidizes cysteines. (A) Intestinal epithelial cells (SKCO15) were contacted with 10^8 CFU/mL of *E. coli* or LGG for 15 min, and then with 15 μM HydroCy3 for 30 min before confocal microscopic analysis at 555 nm, (scale bars 20 μm). (B) SKCO15 were contacted with 10^8 CFU/mL of *E. coli* or LGG for 15 min, labeled for 30 min with a thiol-reactive, Thiol Tracker™ fluorescence probe, and then analyzed by fluorescence microscopy at 405 nm (scale bars 200 μm). Mean image intensity is shown at bottom left for A and B. (C) Biotinylated-iodoacetamide (BIAM) labeling of cysteine residues in lysates of LGG or *E. coli* contacted SKCO15 cells, followed by pull-down of labeled residues with streptavidin conjugated agarose and detected by Western blot using HRP conjugated streptavidin as a probe. The relative intensity of each lane of the blot is shown in arbitrary units to the left. Each value was normalized to calnexin that served as a loading control to give the relative oxidation amounts. (D) Dual labeling of LGG or *E. coli* contacted (15 mins) SKCO15 cultured cells with HydroCy3 (red) and Lysotracker (green). Note co-localization of lysotracker and hydro-Cy3 in LGG contacted cells (bars 10 μm).

lysosomes of IECs after LGG contact may be associated with the stimulation of Nox1 activity that has accumulated in endo/lysosomal vesicles. Increases in lysosomal ROS production in the epithelium after LGG contact might also indicate an increase in protein degradation, thus decreasing the available number of reactive cysteines measurable in our assays. However, routine analysis by Western blot for different epithelial cell proteins after lysis of PBS, LGG or *E.coli* contacted cells did not reveal significant changes in protein levels between treatments when loaded onto gels as microgram or volumetric equivalents (data not shown). Nonetheless, we controlled for the possibility of lysosomal protein degradation in subsequent analysis by using an ICAT double labeling system that measures both the reduced and oxidative cysteines and uses their abundance ratio to normalize and determine the global level of protein oxidation. This is in contrast to the Thiol Tracker™ probe or the BIAM label which only binds reduced forms of the protein, and thus could potentially reflect increases in oxidation that are actually due to loss by degradation instead of the presumed loss of reactivity at an oxidized cysteine.

Thus, to identify the LGG-specific targets of protein oxidation under physiological conditions, we used germ-free mice and the ICAT proteomics technique to asses redox levels at discrete cysteine residues (Fig. 2A). While many studies have used oral gavage to administer probiotics, we chose intra-rectal lavage of germ-free mice, following the procedure used in [2], instead of oral gavage in order to capture the rapid events that occur immediately after bacterial contact with the colonic epithelium, such as would occur in fecal microbiota transplantation. The use of germ-free mice and a short direct contact time were used to maximize the detection of cysteines oxidized by LGG contact. To minimize a bolus of bacterial solution forming in the colon, our lab has developed an inoculation procedure with anesthetized mice that delivers a small volume of bacterial solution (100 ul) that coats but does not inflate the lumen of the colon. After a 15 min rectal lavage of LGG or *E. coli* (10^8 CFU), colonic intestinal scrapings (primarily epithelium) were processed for ICAT analysis. Protein database searches were performed on mouse-specific sequences to minimize detection of bacterial peptides collected in the epithelial scrapings. Consistent with our in vitro findings, the redox levels in the intestinal epithelium of the group receiving rectal LGG lavages were more oxidized than the *E.coli* controls, with LGG having an overall shift in redox potential towards oxidation (Fig. 3B). Our ICAT assay captured ~1500 peptides, of which the majority of peptides had higher levels of oxidation after LGG lavage (compared to *E.coli*) with ~450 of those peptides corresponding to individual proteins that had a fold change of 1.2, and significance of $p < 0.05$ or less (Fig. 3B, Supplemental Table 1). When these peptides are graphed according to their relative percentage of oxidation it is evident that an overall shift in oxidation has occurred in a large set of redox-sensitive proteins in colonic tissue following LGG lavage (Fig. 3C). Thus, ROS production in the epithelium following LGG contact oxidizes a considerable number of cysteine residues in the proteome.

Bioinformatic analysis on the list of redox proteins sensitive to LGG-induced cellular ROS generation (compared to *E. coli* control)

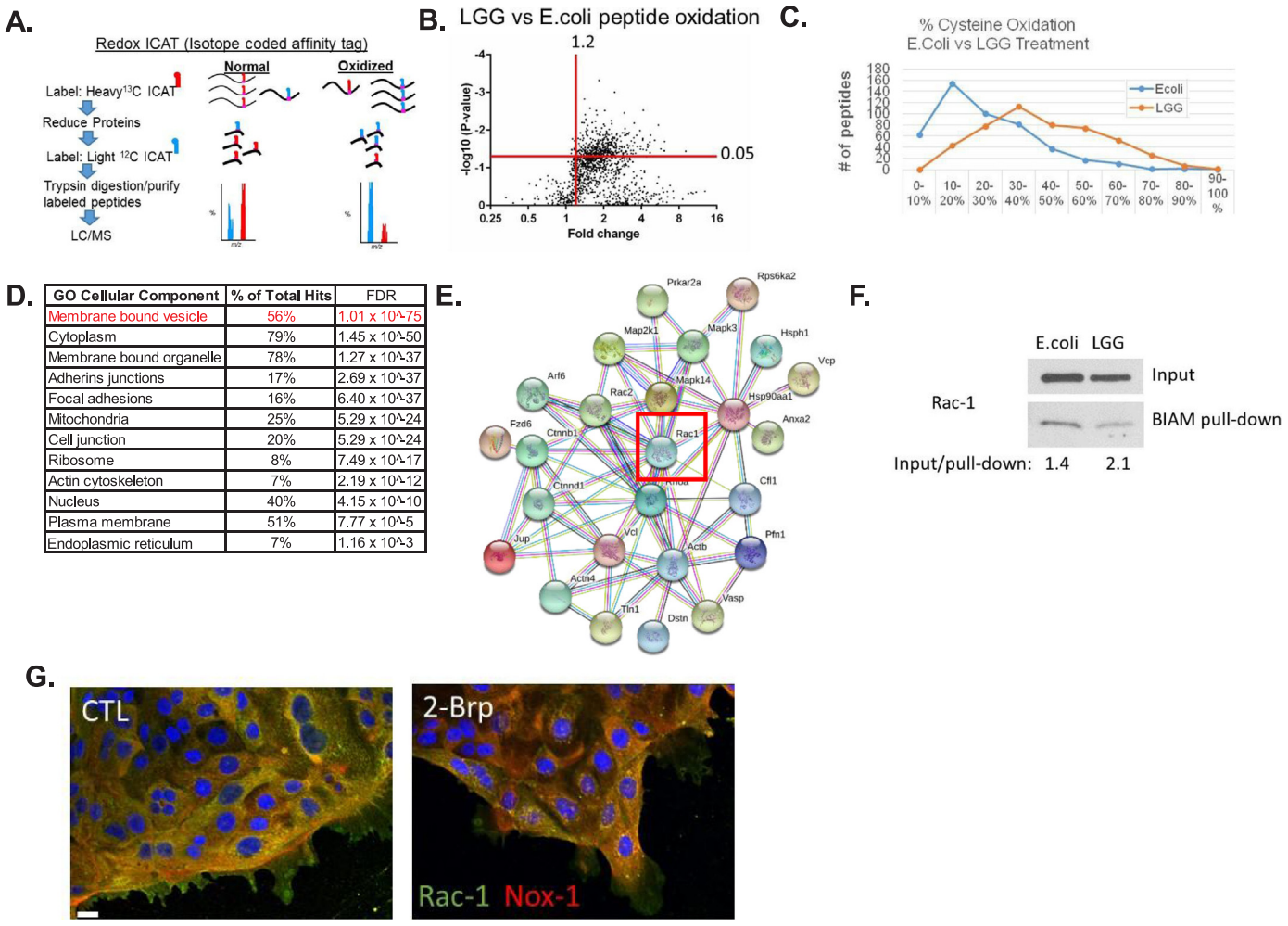

GO Cellular Component	% of Total Hits	FDR
Membrane bound vesicle	56%	1.01 x 10^-75
Cytoplasm	79%	1.45 x 10^-50
Membrane bound organelle	78%	1.27 x 10^-37
Adherins junctions	17%	2.69 x 10^-37
Focal adhesions	16%	6.40 x 10^-37
Mitochondria	25%	5.29 x 10^-24
Cell junction	20%	5.29 x 10^-24
Ribosome	8%	7.49 x 10^-17
Actin cytoskeleton	7%	2.19 x 10^-12
Nucleus	40%	4.15 x 10^-10
Plasma membrane	51%	7.77 x 10^-5
Endoplasmic reticulum	7%	1.16 x 10^-3

Fig. 3. ICAT analysis of intestinal epithelial scrapings from Germ-free mice given a rectal lavage containing 10^8 CFU/mL of LGG or *E. coli* for 15 min (A) Graphical representation of ICAT labeling procedure. (B) Volcano plot of peptide hits (~1500) differentially oxidized in LGG contacted colon compared to *E.coli* contacted colon. (C) Relative peptide oxidation levels significantly changed in LGG or *E.coli* contacted colon. (D) Pathways analysis of peptide hits significantly oxidized in LGG samples (hits from upper right quadrant in A). (E) STRING map of proteins involved in membrane bound vesicle pathway, including Rac1. (F) BIAM labeling of cell lysates from SKCO15 cells after 15 min contact with 10^8 CFU/mL of LGG or *E. coli* for 15 min. Inputs lysates, and pull-down lysates were analyzed by immunoblot using an antibody against Rac1. (G) SKCO15 cells exhibit decreased subcellular co-localization between Rac1 (green) and Nox1 (yellow) after exposed to 25 μM 2-Brp for 2 h, (scale bar μm).

(Supplemental Table 1) using STRING [40] suggest pathways altered by LGG-induced redox changes (Fig. 3D). The full set of cellular components and pathways is listed in Supplemental Table 2. These changes are ranked according to false discovery rate and statistical confidence. We found that proteins that function in membrane bound vesicles ranked at the top for pathways changed upon LGG contact. In accordance with our data showing increases of ROS in lysosomal vesicles (Fig. 2D), it is possible that the membrane bound vesicle subset of proteins may function in Nox1 activity at these locations. Subcellular regions such as cell junctions and focal adhesions, which are important for barrier function and cell migration, respectively, were both significantly impacted by LGG-induced redox changes (Fig. 2D). Indeed, improved barrier function has been shown to occur after LGG administration [10,28,43,5], and the proteins we have identified with ICAT may be key mediators in these processes.

Given the role of Nox1 in LGG-induced ROS generation in the epithelium, we found the changes in membrane bound vesicles after LGG stimulation to be most interesting, especially because ROS production by Nox1 is controlled by its endocytosis, and involves clustering with Rac1 [15]. Nox1 activity is regulated by Rac1 and our ICAT analysis identified a peptide for Rac1 that was significantly oxidized at residue C178 after exposure to LGG (Supplemental Table 1). STRING analysis on the subset of proteins with functions related to membrane bound vesicles is shown in Fig. 2E. To validate these findings, the redox state of Rac1 was measured using a BIAM cysteine pull down assay in SKCO15 cells after contact with LGG or *E.coli* for 15-min (Fig. 2C). Blotting analysis revealed higher levels of Rac1 oxidation in the LGG contacted cells than the *E.coli* control (Fig. 3F). Compared to *E.coli* treated cells, densitometry analysis revealed a 1.5 fold increase in Rac1 oxidation in LGG treated SKCO15 cells.

Rac1 localization to the plasma membrane has been shown to be controlled by palmitoylation of its C178 residue [33]. Accumulation of Rac1 at the plasma membrane places it in sub-cellular proximity to Nox1, where Rac1 functions as the activating switch for ROS production by Nox1. Indeed, inhibition of cellular protein palmitoylation with 2-Brp decreased the co-localization of Rac1 and Nox1 at the leading edge of SKCO15 monolayers (Fig. 3G). Together, these data infer the compelling notion that oxidation of Rac1 likely functions in down regulating Nox1 activity soon after contact of the epithelium with LGG; a step likely required to dampen the pernicious effects of overt ROS generation on cellular macromolecules. Our projected model suggests that palmitoylation of Rac1 at C178 and its subsequent activation is increased in an FPR-dependent manner [4] in the presence of LGG, and then recruited to the plasma membrane in close proximity of Nox1.

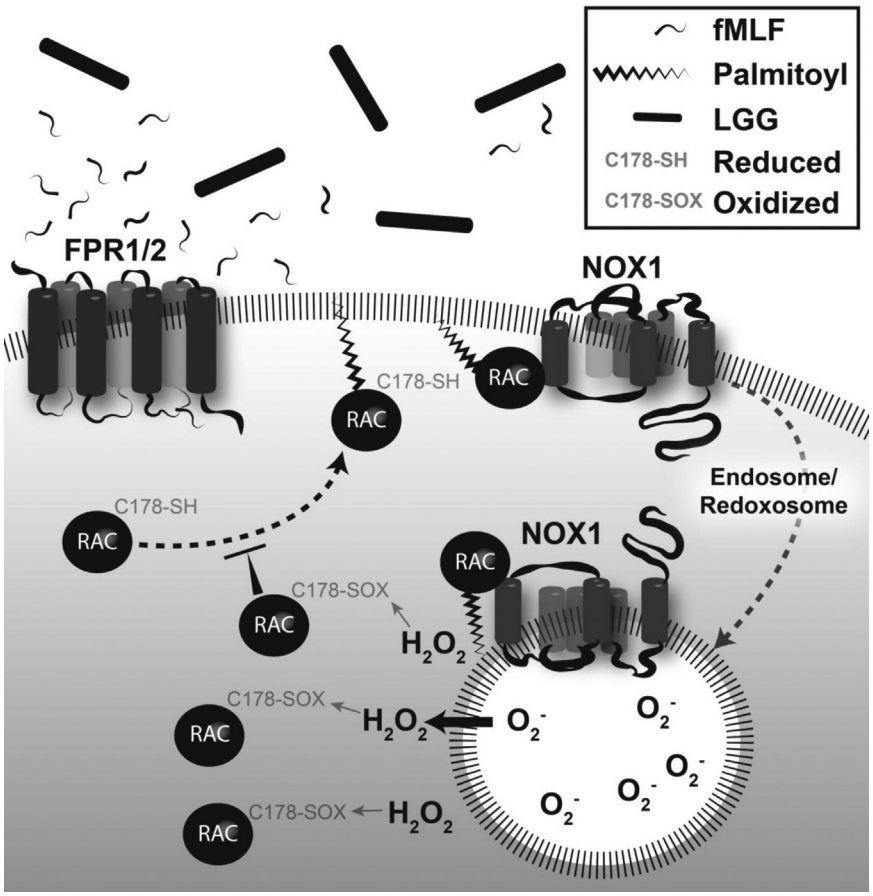

Fig. 4. Putative model for LGG regulation of ROS production in the gut epithelium. Rac1 is first activated following LGG stimulation of Formyl Peptide Receptor. Rac1 subsequently becomes palmitoylated at C178 and localized at the plasma membrane, where it activates Nox-1 to generate ROS. Endocytosis of this complex forms a redoxosome that generates elevated levels of ROS. In a feedback loop, further palmitoylation of Rac-1 is blocked by oxidation of C178, decreasing the formation of redoxosomes.

Both Rac1 and Nox1 are then endocytosed into the cytosol to form a redoxosome. The subsequent redoxosome generated ROS burst then oxidizes pools of Rac1 at C178 that would otherwise be palmitoylated, thereby functioning as a feedback mechanism to prevent further plasma membrane accumulation of Rac1 with Nox1. This would have the net effect of down regulating further redoxosome/ROS generation (Fig. 4). This controlled fluctuation in ROS levels and subsequent oxidation of mucosal proteins, particularly of Rac1, sheds new light on the mechanisms of regulating ROS production in the intestinal epithelium after exposure to LGG, and the proteins oxidized and regulated that underlie the signaling that gives rise to the beneficial properties of LGG in modulating intestinal homeostasis.

3. Methods

3.1. Germ-free animals

Germ-free mice were purchased from the Emory Gnotobiotic Animal Core (EGAC). EGAC is supported by the Georgia Clinical & Translational Science Alliance and the Emory University School of Medicine.

3.2. Cells, antibodies and reagents

Intestinal epithelial cells SKCO15 were a kind gift from Dr. Charles Parkos, and were maintained in high glucose DMEM containing 10% fetal bovine serum, additionally supplemented with non-essential amino acids and L-glutamine. The mouse Rac-1 antibody was purchased from BD Transduction. The HydroCy3 was obtained from LI-Core (sold as ROSstar 550), and the Thiol Tracker from Thermo Scientific and were both used as directed in the manufacturers' instructions and images acquired using a standard fluorescence microscope with camera. The biotinylated iodoacetamide was obtained from Anaspec. Anti-mouse secondary antibody conjugated to HRP was obtained from GE, while the streptavidin conjugated HRP was obtained from Abcam. Rabbit anti-calnexin was purchased from Sigma-Aldrich. ROS-GLO assay was purchased from Promega and performed in a 96-well format following the manufacturer's instructions on overnight cultures of bacterial supernatants.

3.3. Bacterial Strains and intra-rectal lavage

Escherichia coli K-12 DH5α and *Lactobacillus rhamnosus* GG lab strain 1 (ATCC 53103), *Lactobacillus sakei supsp. sakei* (ATCC 15521), *Lactobacillus rhamnosus* lab strain 2 (ATCC 53103), *Lactobacillus gasseri* (ATCC 19992), *Lactobacillus plantarum* (ATCC 14917), , *Lactobacillus acidophilus* (ATCC 4356) were obtained from American Type Culture Collection (ATCC) and propagated in LB for *E.coli* and the Lactobacilli strains cultured in MRS media. For the redox assays, after overnight growth, *E.coli* and LGG cultures were pelleted by centrifugation, and the pellet washed with PBS. After spectrophotometric density determination at 600 nm, the bacteria were resuspended in PBS to a population density of 10^6 CFU/μL. Thereafter, an appropriate quantity of culture liquid (100 μL) was injected intra-rectally per anesthetized mouse, or 10^8 CFU/mL in cell media when applied to intestinal epithelial cells grown in vitro.

Anesthetized (ketamine/xylazine) mice intra-rectally injected with bacterial solution where placed in a slanted nose-down position to maintain colonic bacterial contact without leakage for 15-min. Colonic scrapings were prepared by colonic resection and dissection to remove luminal contents by PBS wash and mechanical dislodging. Scrapings were prepared by running the edge of a clean microscope slide down the exposed surface of the colonic mucosa and the scrapings collected into a microcentrifuge tube and snap frozen in liquid nitrogen.

Databases using mouse sequences were used to analyze the extracts, which also excluded the detection of bacterially derived proteins in the MS/MS analysis (see details below).

3.4. Isotope-coded affinity tags (ICAT) and MS/MS analysis

The Cleavable ICAT® Reagent for Protein Labeling (SKU #: 4339036) was purchased from SCIEX (Framingham, MA). The ICAT and MS/MS analysis was performed as described previously [12,13]. Briefly, trichloroacetic acid (TCA) precipitated proteins from cell lysates were incubated with a heavy ICAT reagent to label reduced cysteines, followed by a second TCA precipitation, reduction with TCEP, and then labeling of newly reduced cysteines with a light ICAT reagent. Following overnight trypsin digestion and an on column purification (1st round anion exchange, second round streptavidin) of biotinylated peptides with heavy and light labels, samples were vacuum-dried before processing. Derived peptides were resuspended in peptide 20 µL of loading buffer (0.1% formic acid, 0.03% TFA, 1% acetonitrile). Peptide mixtures (5 µL) were separated on a self-packed C18 (1.9 µm Dr. Maisch, Germany) fused silica column (25 cm × 75 uM internal diameter (ID); New Objective, Woburn, MA) by a Dionex Ultimate 3000 RSLCNano and monitored on a Fusion mass spectrometer (ThermoFisher Scientific , San Jose, CA). Elution was performed over a 120 min gradient at a rate of 300 nl/min with buffer B ranging from 3% to 65% (buffer A: 0.1% formic acid in water, buffer B: 0.1% formic in acetonitrile). The mass spectrometer cycle was programmed to collect at the top speed for 3 s cycles. The MS scans (400–1600 m/z range, 200,000 AGC, 50 ms maximum ion time) were collected at a resolution of 120,000 at m/z 200 in profile mode while the HCD MS/MS spectra (0.7 m/z isolation width, 30% collision energy, 10,000 AGC target, 35 ms maximum ion time) in centroid mode were detected in the ion trap. Dynamic exclusion was set to exclude previous sequenced precursor ions for 20 s within a 10 ppm window. Precursor ions with +1, and + 8 or higher charge states were excluded from sequencing. Raw files were searched using Proteome Discoverer version 2.0.0.802 (ThermoFisher) against a mouse database downloaded from NCBI REFSEQ project (version 62 with 30,267 target sequences). Search parameters include fully tryptic restriction, a parent ion mass tolerance (± 20 ppm), a product ion mass tolerance of 0.6 Da and a miscleavage allowance of 2. Methionine oxidation (+15.9949 Da), asparagine and glutamine deamidation (+0.9840 Da), protein N-terminal acetylation (+42.0106 Da), cysteine light ICAT (+227.12699) and cysteine heavy ICAT (+236.15719) were variable modifications (up to 5 allowed per peptide). Percolator was used to filter the peptide spectrum matches to a false discovery rate of 1%.

3.4.1. Redox pull-down assay

Stimulated epithelial cell monolayers were lysed in tris-buffered saline containing 1% Triton X-100 and the insoluble material was removed by centrifugation. Samples were adjusted to 25 µM (biotinylated iodoacetamide) BIAM and incubated on ice in the dark for 45 min. Labeled proteins were separated from free BIAM label by passage through a Zeba Spin Desalting Column, (7K MWCO) (Product # 89882) (Thermo Fischer Scientific), and immobilized onto streptavidin agarose for 1 h. After extensive washing the proteins were released from the streptavidin agarose by 1% SDS and 95 °C heat for 5 min. SDS-PAGE and Western blotting were performed on the samples using standard techniques.

3.4.2. Immunostaining

Rac1 and Nox1 were visualized by fluorescence microscopy on an Olympus FV1000 Confocal microscope. Cell were placed in cold formaldehyde fixation and saponin permeabilized prior to incubation with mouse anti-Rac1 (BD Transduction) and Rabbit anti-Nox-1 (Sigma). Primary antibodies were detected with secondary anti-mouse Alexa 488 and anti-rabbit Alexa 555. DNA was visualized using DAPI staining.

3.4.3. Statistics

Biological triplicates of ICAT tagged peptides from each treatment group (LGG gavaged vs. *E. coli*) were subjected to the following statistical analyses. Total peptides (10,923 peptides) that had detectable label in no less than 2 of the triplicates (1364) were further statistically analyzed. A Kruskal-Wallis non-parametric multiple comparisons analyses showed that the medians of the LGG and *E. coli* gavaged treatment groups significantly differed $p < 0.05$. Dunn's post-hoc analyses of multiple rank comparisons did not reveal any outlier groups (as defined by 3 standard deviations from the mean). LGG and *E. coli* data were grouped and analyzed by a 2-way ANOVA. Significant variation was observed for LGG vs. *E. coli* as well as peptides vs peptides ($p < 0.0001$). Grouped *t*-tests were performed to determine 486 significant hits at $p < 0.05$.

Acknowledgments

The Emory Integrated Proteomics Core (EIPC)

Competing interests

The authors declare no competing financial interests.

Funding

JDM is funded by a Crohn's and Colitis Foundation of America (CCFA, CDA#451678). TMD is funded by a Crohn's and Colitis Foundation of America (CCFA). RMJ is supported in part by NIH Grant RO1 CA179424 and R01DK098391. ASN is supported, in part, by NIH R01DK071604 and RO1AI064462. ARR is funded by T32DK007771-06 training grant. BRR is funded by T32DK108735-03 training grant.

Appendix A. Supporting information

Supplementary data associated with this article can be found in the online version at doi:10.1016/j.redox.2018.11.011.

References

[1] M.C. Abt, P.T. Mckenney, E.G. Pamer, Clostridium difficile colitis: pathogenesis and host defence, Nat. Rev. Microbiol. 14 (2016) 609–620.
[2] A. Alam, G. Leoni, M. Quiros, H. Wu, C. Desai, H. Nishio, R.M. Jones, A. Nusrat, A.S. Neish, The microenvironment of injured murine gut elicits a local pro-restitutive microbiota, Nat. Microbiol. 1 (2016) 15021.
[3] A. Alam, G. Leoni, C.C. Wentworth, J.M. Kwal, H. Wu, C.S. Ardita, P.A. Swanson, J.D. Lambeth, R.M. Jones, A. Nusrat, A.S. Neish, Redox signaling regulates commensal-mediated mucosal homeostasis and restitution and requires formyl peptide receptor 1, Mucosal Immunol. 7 (2014) 645–655.
[4] B.A. Babbin, A.J. Jesaitis, A.I. Ivanov, D. Kelly, M. Laukoetter, P. Nava, C.A. Parkos, A. Nusrat, Formyl peptide receptor-1 activation enhances intestinal epithelial cell restitution through phosphatidylinositol 3-kinase-dependent activation of Rac1 and Cdc42, J. Immunol. 179 (2007) 8112–8121.
[5] R.C. Chen, L.M. Xu, S.J. Du, S.S. Huang, H. Wu, J.J. Dong, J.R. Huang, X.D. Wang, W.K. Feng, Y.P. Chen, Lactobacillus rhamnosus GG supernatant promotes intestinal barrier function, balances Treg and TH17 cells and ameliorates hepatic injury in a mouse model of chronic-binge alcohol feeding, Toxicol. Lett. 241 (2016) 103–110.
[6] H. Choi, A. Dikalova, R.J. Stark, F.S. Lamb, c-Jun N-terminal kinase attenuates TNFalpha signaling by reducing Nox1-dependent endosomal ROS production in vascular smooth muscle cells, Free Radic. Biol. Med. 86 (2015) 219–227.
[7] S.P. Costello, M.A. Conlon, M.S. Vuaran, I.C. Roberts-Thomson, J.M. Andrews, Faecal microbiota transplant for recurrent Clostridium difficile infection using long-term frozen stool is effective: clinical efficacy and bacterial viability data, Aliment Pharmacol. Ther. 42 (2015) 1011–1018.
[8] J. Digby-Bell, A. Williams, P. Irving, S. Goldenberg, Successful faecal microbiota transplant for recurrent Clostridium difficile infection delivered by colonoscopy through a diverted ileostomy in a patient with severe perianal Crohn's disease, BMJ Case Rep. (2018) 2018.
[9] K.A. Donato, M.G. Gareau, Y.J. Wang, P.M. Sherman, Lactobacillus rhamnosus GG attenuates interferon-{gamma} and tumour necrosis factor-alpha-induced barrier dysfunction and pro-inflammatory signalling, Microbiology 156 (2010) 3288–3297.
[10] C.B. Forsyth, A. Farhadi, S.M. Jakate, Y. Tang, M. Shaikh, A. Keshavarzian, Lactobacillus GG treatment ameliorates alcohol-induced intestinal oxidative stress, gut leakiness, and liver injury in a rat model of alcoholic steatohepatitis, Alcohol 43 (2009) 163–172.

[11] Y.M. Go, J. Pohl, D.P. Jones, Quantification of redox conditions in the nucleus, Methods Mol. Biol. 464 (2009) 303–317.
[12] Y.M. Go, J.R. Roede, M. Orr, Y. Liang, D.P. Jones, Integrated redox proteomics and metabolomics of mitochondria to identify mechanisms of cd toxicity, Toxicol. Sci. 139 (2014) 59–73.
[13] Y.M. Go, J.R. Roede, D.I. Walker, D.M. Duong, N.T. Seyfried, M. Orr, Y. Liang, K.D. Pennell, D.P. Jones, Selective targeting of the cysteine proteome by thioredoxin and glutathione redox systems, Mol. Cell Proteom. 12 (2013) 3285–3296.
[14] V. Gopalakrishnan, B.A. Helmink, C.N. Spencer, A. Reuben, J.A. Wargo, The influence of the gut microbiome on cancer, immunity, and cancer immunotherapy, Cancer Cell 33 (2018) 570–580.
[15] M.M. Harraz, J.J. Marden, W. Zhou, Y. Zhang, A. Williams, V.S. Sharov, K. Nelson, M. Luo, H. Paulson, C. Schoneich, J.F. Engelhardt, SOD1 mutations disrupt redox-sensitive Rac regulation of NADPH oxidase in a familial ALS model, J. Clin. Investig. 118 (2008) 659–670.
[16] R.M. Jones, The influence of the gut microbiota on host physiology: in pursuit of mechanisms, Yale J. Biol. Med. 89 (2016) 285–297.
[17] R.M. Jones, C. Desai, T.M. Darby, L. Luo, A.A. Wolfarth, C.D. Scharer, C.S. Ardita, A.R. Reedy, E.S. Keebaugh, A.S. Neish, Lactobacilli modulate epithelial cytoprotection through the Nrf2 pathway, Cell Rep. 12 (2015) 1217–1225.
[18] R.M. Jones, L. Luo, C.S. Ardita, A.N. Richardson, Y.M. Kwon, J.W. Mercante, A. Alam, C.L. Gates, H. Wu, P.A. Swanson, J.D. Lambeth, P.W. Denning, A.S. Neish, Symbiotic lactobacilli stimulate gut epithelial proliferation via Nox-mediated generation of reactive oxygen species, EMBO J. 32 (2013) 3017–3028.
[19] R.M. Jones, J.W. Mercante, A.S. Neish, Reactive oxygen production induced by the gut microbiota: pharmacotherapeutics implications, Curr. Med. Chem. 19 (2012) 1519–1529.
[20] R.M. Jones, A.S. Neish, Redox signaling mediated by the gut microbiota, Free Radic. Biol. Med. 105 (2017) 41–47.
[21] C. Klomsiri, L.C. Rogers, L. Soito, A.K. Mccauley, S.B. King, K.J. Nelson, L.B. Poole, L.W. Daniel, Endosomal H_2O_2 production leads to localized cysteine sulfenic acid formation on proteins during lysophosphatidic acid-mediated cell signaling, Free Radic. Biol. Med. 71 (2014) 49–60.
[22] E. Kobatake, H. Nakagawa, T. Seki, T. Miyazaki, Protective effects and functional mechanisms of Lactobacillus gasseri SBT2055 against oxidative stress, PLoS One 12 (2017) e0177106.
[23] E. Kolaczkowska, P. Kubes, Neutrophil recruitment and function in health and inflammation, Nat. Rev. Immunol. 13 (2013) 159–175.
[24] H. Kruger, G. Bauer, Lactobacilli enhance reactive oxygen species-dependent apoptosis-inducing signaling, Redox Biol. 11 (2017) 715–724.
[25] M.R. Kudelka, B.H. Hinrichs, T. Darby, C.S. Moreno, H. Nishio, C.E. Cutler, J.M. Wang, H.X. Wu, J.W. Zeng, Y.C. Wang, T.Z. Ju, S.R. Stowell, A. Nusrat, R.M. Jones, A.S. Neish, R.D. Cummings, Cosmc is an X-linked inflammatory bowel disease risk gene that spatially regulates gut microbiota and contributes to sex-specific risk, Proc. Natl. Acad. Sci. USA 113 (2016) 14787–14792.
[26] J.D. Lambeth, A.S. Neish, Nox enzymes and new thinking on reactive oxygen: a double-edged sword revisited, Annu. Rev. Pathol. 9 (2014) 119–145.
[27] G. Leoni, A. Alam, P.A. Neumann, J.D. Lambeth, G. Cheng, J. Mccoy, R.S. Hilgarth, K. Kundu, N. Murthy, D. Kusters, C. Reutelingsperger, M. Perretti, C.A. Parkos, A.S. Neish, A. Nusrat, Annexin A1, formyl peptide receptor, and NOX1 orchestrate epithelial repair, J. Clin. Investig. 123 (2013) 443–454.
[28] J.Y. Li, B. Chassaing, A.M. Tyagi, C. Vaccaro, T. Luo, J. Adams, T.M. Darby, M.N. Weitzmann, J.G. Mulle, A.T. Gewirtz, R.M. Jones, R. Pacifici, Sex steroid deficiency-associated bone loss is microbiota dependent and prevented by probiotics, J. Clin. Investig. 126 (2016) 2049–2063.
[29] Q. Li, Y. Zhang, J.J. Marden, B. Banfi, J.F. Engelhardt, Endosomal NADPH oxidase regulates c-Src activation following hypoxia/reoxygenation injury, Biochem. J. 411 (2008) 531–541.
[30] F.J. Miller, X. Chu JR., B. Stanic, X. Tian, R.V. Sharma, R.L. Davisson, F.S. Lamb, A differential role for endocytosis in receptor-mediated activation of Nox1, Antioxid. Redox Signal 12 (2010) 583–593.
[31] F.J. Miller, J.R. Filali, M. Huss, G.J. Stanic, B. Chamseddine, A. Barna, T. J, F.S. Lamb, Cytokine activation of nuclear factor kappa B in vascular smooth muscle cells requires signaling endosomes containing Nox1 and ClC-3, Circ. Res. 101 (2007) 663–671.
[32] B.H. Mullish, M.N. Quraishi, J.P. Segal, V.L. Mccune, M. Baxter, G.L. Marsden, D.J. Moore, A. Colville, N. Bhala, T.H. Iqbal, C. Settle, G. Kontkowski, A.L. Hart, P.M. Hawkey, S.D. Goldenberg, H.R.T. Williams, The use of faecal microbiota transplant as treatment for recurrent or refractory Clostridium difficile infection and other potential indications: joint British Society of Gastroenterology (BSG) and Healthcare Infection Society (HIS) guidelines, Gut 67 (2018) 1920–1941.
[33] I. Navarro-Lerida, S. Sanchez-Perales, M. Calvo, C. Rentero, Y. Zheng, C. Enrich, M.A. Del Pozo, A palmitoylation switch mechanism regulates Rac1 function and membrane organization, EMBO J. 31 (2012) 534–551.
[34] A.S. Neish, R.M. Jones, Redox signaling mediates symbiosis between the gut microbiota and the intestine, Gut Microbes 5 (2014) 250–253.
[35] F.D. Oakley, D. Abbott, Q. Li, J.F. Engelhardt, Signaling components of redox active endosomes: the redoxosomes, Antioxid. Redox Signal 11 (2009) 1313–1333.
[36] Y. Seenappanahalli Nanjundaiah, D.A. Wright, A.R. Baydoun, W.T. O'hare, Z. Ali, Z. Khaled, M.H. Sarker, Lactobacillus rhamnosus GG conditioned media modulates acute reactive oxygen species and nitric oxide in J774 murine macrophages, Biochem. Biophys. Rep. 6 (2016) 68–75.
[37] A.K. Singh, R.Y. Hertzberger, U.G. Knaus, Hydrogen peroxide production by lactobacilli promotes epithelial restitution during colitis, Redox Biol. 16 (2018) 11–20.
[38] N.Y. Spencer, J.F. Engelhardt, The basic biology of redoxosomes in cytokine-mediated signal transduction and implications for disease-specific therapies, Biochemistry 53 (2014) 1551–1564.
[39] P.A. Swanson, 2Nd, A. Kumar, S. Samarin, M. Vijay-Kumar, K. Kundu, N. Murthy, J. Hansen, A. Nusrat, A.S. Neish, Enteric commensal bacteria potentiate epithelial restitution via reactive oxygen species-mediated inactivation of focal adhesion kinase phosphatases, Proc. Natl. Acad. Sci. USA 108 (2011) 8803–8808.
[40] D. Szklarczyk, J.H. Morris, H. Cook, M. Kuhn, S. Wyder, M. Simonovic, A. Santos, N.T. Doncheva, A. Roth, P. Bork, L.J. Jensen, C. Von Mering, The STRING database in2017: quality-controlled protein-protein association networks, made broadly accessible, Nucleic Acids Res. 45 (2017) D362–D368.
[41] C.C. Wentworth, A. Alam, R.M. Jones, A. Nusrat, A.S. Neish, Enteric commensal bacteria induce extracellular signal-regulated kinase pathway signaling via formyl peptide receptor-dependent redox modulation of dual specific phosphatase 3, J. Biol. Chem. 286 (2011) 38448–38455.
[42] C.C. Wentworth, R.M. Jones, Y.M. Kwon, A. Nusrat, A.S. Neish, Commensal-Epithelial Signaling Mediated via Formyl Peptide Receptors, Am. J. Pathol. 177 (2010) 2782–2790.
[43] J. Wu, K. Yang, W. Wu, Q. Tang, Y. Zhong, G. Gross, T.T. Lambers, E.A.F. Van Tol, W. Cai, Soluble mediators From Lactobacillus rhamnosus Gorbach-Goldin support intestinal barrier function in rats After massive small-bowel resection, JPEN J. Parenter. Enter. Nutr. 42 (2018) 1026–1034.
[44] F. Yan, H. Cao, T.L. Cover, R. Whitehead, M.K. Washington, D.B. Polk, Soluble proteins produced by probiotic bacteria regulate intestinal epithelial cell survival and growth, Gastroenterology 132 (2007) 562–575.